Advances in Science and Technology Research Journal, 2025, 19(12), 156–172 https://doi.org/10.12913/22998624/209987 ISSN 2299-8624, License CC-BY 4.0

# Polyoxymethylene copolymer matrix nanocomposites with enhanced ability to dissipate mechanical energy

Paulina Kaczor<sup>1</sup>, Stanisław Kuciel<sup>2</sup>, Karina Rusin-Żurek<sup>1</sup>, Patrycja Bazan<sup>2\*</sup>

- <sup>1</sup> Faculty of Material Engineering and Physics, CUT Doctoral School, Cracow University of Technology, 31-155 Kraków, Poland
- <sup>2</sup> Faculty of Material Engineering and Physics, Cracow University of Technology, Warszawska 24, 31-155 Kraków, Poland
- \* Corresponding author's e-mail: patrycja.bazan@pk.edu.pl

#### **ABSTRACT**

The objective of this study was to examine the mechanical properties and surface characteristics of composites with antibacterial potential, specifically those based on structural polyoxymethylene and titanium oxide. The nanocomposite was modified through the incorporation of commercially available impact modifiers derived from high-molecular-weight silicones, as well as aramid fibers with a compatibilizer of ethylene-n-octene grafted with maleic anhydride (EOC-g\_MAH). Fundamental strength and low-cycle tests were conducted to ascertain the dissipation energy of the material, and assessments of surface tension as well as contact angle were performed. The inclusion of silicone was found to diminish the strength properties, yet it positively influenced the release and surface tension of the material. In contrast, aramid fibers enhanced impact strength while reducing the surface contact angle by approximately 6%.

**Keywords:** polyoxymethylene, antibacterial composites, compatibilizer, aramid fiber, silicone masterbatch, mechanical properties, contact angle.

## **INTRODUCTION**

Polyoxymethylene is frequently utilized in the medical and laboratory sectors due to its superior mechanical properties and high resistance to chemical agents [1]. A discernible trend in current research involves the exploration of antibacterial nanocomposites based on a polyoxymethylene resin matrix [2-4]. Metal and metal oxide nanoparticles, such as Ag, Au, Cu, Se, Ag-Au, Ag-Ti, Ag<sub>2</sub>O, ZnO, CuO, TiO<sub>2</sub>, SiO<sub>2</sub>, MgO, and MgO<sub>3</sub>, are primarily identified as modifiers with biocidal potential [5–7]. A 2023 study assessing the biocidal efficacy of metal nanoparticles and metal oxides, including Ag, ZnO, TiO2, and CuO, incorporated into POM at a concentration of 2% wt.%, determined that the POM + TiO, 2% composite exhibited the highest antibacterial activity. However, the inclusion of 2% nanoparticles resulted in a decline in mechanical properties, with a 7% reduction in flexural strength and a 3% reduction in elastic modulus, respectively. Additionally, tensile strength and Young's modulus experienced a reduction of approximately 2–3%. The impact strength of these composites also diminished [4]. Consequently, an investigation was initiated to enhance the POM + TiO<sub>2</sub> 2% antimicrobial composite, aiming to minimize the loss of desirable mechanical properties, with a particular focus on improving the impact properties of the composite.

Received: 2025.07.13

Accepted: 2025.10.01

Published: 2025.11.01

The most frequently utilized modifiers that enhance the mechanical properties of polyoxymethylene (POM) include glass fibers, basalt fibers, glass beads, carbon fibers, and aramid fibers [1]. Chenghe Liu et al. investigated the incorporation of short basalt fibers at a weight content of 20%, which resulted in improvements in tensile strength by 27.45%, flexural strength by 18.11%, and impact strength by 9.65% [8]. Yatao Wang et al. examined composites reinforced with long

basalt fibers, achieving materials with superior mechanical and impact properties [9]. Wenzhong et al. observed that the addition of carbon fibers at 5, 10, 15, and 20 wt% led to increases in tensile strength and Young's modulus, as well as enhancements in flexural strength and flexural modulus with higher percentages of addition. However, a decrease in mechanical strength was noted with the addition of up to 5 wt%. Impact strength began to increase after the addition of 10 wt% and more, which can be attributed to the fracture transformation mechanism [10]. A similar correlation regarding carbon fibers and their effect on mechanical properties was reported by Tang et al. [11]. Pıhtılı and Tosun investigated composites based on aramid and glass fibers, demonstrating that the mechanical properties of the former were significantly superior [12]. Luo et al. demonstrated that the addition of aramid fibers in amounts of 5, 10, and 15% by weight improved mechanical properties, with a 15% by weight addition increasing tensile strength by 43% and impact strength by 23% [13]. The effectiveness of aramid fiber reinforcement can depend on several factors, including the quantity, distribution, shape, length, and, most importantly, the adhesion of the fibers to the polymer matrix [14–16]. It has been noted that in fiber-reinforced thermoplastic materials, the adhesion of fibers to the polymer matrix is crucial for enhancing the mechanical properties of the composites [17]. Additionally, previous fiber treatment and surface morphology have been shown to significantly impact matrix compatibility [18–20]. Polytetrafluoroethylene (PTFE) is a commonly utilized polymer additive for reducing friction and wear. It is recommended as a compatibilizer in the composites containing aramid fibers and other types of fibers [21–23]. Additionally, maleic anhydride grafted ethylene n-octene (EOC-g MAH) has been employed as a compatibilizer for polyoxymethylene and basalt fibers [24], it can also be used independently to enhance the dynamic impact resistance of PET [25]. Afsaneh Fakhar et al. investigated polyoxymethylene (POM) composites with the incorporation of 20 wt% short aramid fibers and 13 wt% PTFE particles. Aramid fibers have been demonstrated to enhance the elastic modulus and tensile strength [22]. The incorporation of small quantities of ethylene propylene diene elastomers (EPDM) and a low-modulus ethylene-vinyl acetate (EVA) copolymer results in increased impact strength, leading to a compound with superior

mechanical and impact properties [26, 27]. Mehrabzadeh et al. reported the beneficial effect of a thermoplastic polyurethane elastomer [28], while Uthaman highlighted the impact of ethylene-vinyl acetate copolymer on material impact strength [27]. Gowda et al. observed that PTFE usage improved impact strength by approximately 20% without notching, attributed to the dissipation of impact energy by the ductile silicone phase and soft PTFE [29]. Palanivelu K et al. documented a significant enhancement in impact strength following the addition of thermoplastic polyurethane [30], and Gao, Yang et al. noted a slight improvement in the impact strength of POM/PTFE composites, which was markedly enhanced by the addition of PEO [31]. However, some studies emphasize the issue of PTFE-based additives tending to agglomerate, posing challenges for uniform distribution in high-viscosity polymers. Poor adhesion between polyoxymethylene and PTFE can lead to the deterioration of the mechanical properties of POM/PTFE composites [32]. Furthermore, certain studies highlight the issue of compatibility between the POM matrix and most rubber modifiers, which may adversely affect mechanical properties and significantly degrade impact resistance [33, 34]. The hydrophilicity and hydrophobicity of solid surfaces are crucial properties for both fundamental research and practical applications. The contact angle serves as a convenient metric for assessing the wettability of a solid surface, being sensitive to alterations in surface properties. These alterations may result from physical, chemical, or physicochemical factors [35]. Research suggests that antibacterial properties are correlated with surface characteristics, and an increase in the contact angle positively influences biocidal activity [36, 37]. This is attributed to the fact that when a surface is contaminated with bacteria, three distinct stages can be identified: the adhesion phase, the colonization phase, and the proliferation phase. Consequently, it can be inferred that hydrophobic materials exhibit enhanced antimicrobial potential due to reduced surface adhesion [38].

The objective of this study was to develop and characterize advanced POM nanocomposites with synergistic dynamic and surface properties, suitable for use in medical equipment components that require enhanced resistance to mechanical damage and reduced adhesion of biological contaminants. The research conducted confirms that a carefully selected combination of silicone modifiers, aramid

fibers, and a compatibilizer within a POM copolymer matrix, supplemented with TiO2 nanoparticles, results in a material with optimized mechanical properties-specifically, increased resistance to dynamic loads and enhanced energy dissipation capacity—while potentially maintaining antibacterial properties. Several aspects underscore the innovative nature of this research. Notably, the integration of dynamic energy dissipation analysis (hysteresis loops) with the evaluation of the hydrophobicity of POM composites, modified concurrently with TiO2 nanoparticles, aramid fibers, and high-molecular silicones, demonstrates that the appropriate morphology of aramid fibers and their compatibilization within the POM matrix significantly influence the ability of the material to dampen mechanical energy and resist shock loads. Furthermore, it has been confirmed that the increase in contact angle due to silicone modifiers correlates with an enhanced release potential, which is crucial for reducing surface colonization by microorganisms, thereby potentially maintaining and improving antibacterial properties. This work aligns with the current trend of seeking materials that synergistically combine mechanical and functional properties (antibacterial and hydrophobic), offering added value beyond previous studies that primarily focused on static reinforcement or solely the biocidal effect. These findings could serve as a foundation for further industrial and application research, particularly in the domain of medical and laboratory components with extended service life and increased biological resistance.

**Table 1.** Characteristic properties of polyoxymethylene Tarnoform 500 CE

Dranatica	Tarnoform		
Properties	500 CE		
Density [kg/m³]	1410		
Melt volume rate, MVR 230 °C /2.16 kg	24		
[cm <sup>3</sup> /10 min]			
Tensile modulus [MPa]	2800		
Tensile stress at yeld, 50 mm/min [MPa]	64		
Flexural modulus, 23 °C [MPa]	2550		
Melting temperature [°C]	166		

#### **MATERIALS AND METHODS**

# Preparation of materials and composites

Polyoxymethylene copolymer (POM-C), commercially known as Tarnoform 500 CE, was utilized as the matrix material (Celanese Corporation, Irving, TX, USA). Table 1 delineates the characteristic properties of the pure polymer. According to the research conducted [4], antibacterial composites were developed using a polyoxymethylene matrix with the incorporation of 2 wt% Titanium (IV) oxide, 98+%, anatase powder, Size: <1000 ppm (1 nm), produced by Acros Organics B.V.B.A., a division of Thermo Fisher Scientific (Waltham, MA, USA). The samples were fabricated in accordance with ISO 3167:2002 [39] utilizing the KM 40–125 Winner Krauss. Table 2 outlines the processing parameters employed. The composites were modified through the addition of high molecular weight silicones, aramid fibers, and impact compatibilizers. The composites were produced without prior compounding. Prior to the injection process, the materials were dried, the dry ingredients were weighed, and subsequently introduced into the hopper of the injection molding machine in small quantities. Table 3 provides a comprehensive description of the produced samples.

Aramid fibers were selected for the preparation of the composites. Aramid fibres are widely recognized as effective in increasing the impact strength of polymer composites due to their high energy absorption and stress dissipation capacity. Chen et al. demonstrated that the incorporation of aramid fibers into polyurethane-epoxy composites significantly enhances both tensile strength and impact strength [39]. Similarly, in hybrid systems, Pincheira et al. reported a 37.9% increase in energy absorption [40], and Overberg et al. reported a 70% increase in impact strength compared to carbon fiber-only reinforced composites [41]. Aramid nanofibers have additional benefits — Du et al. observed an increase in impact strength of 81.8% with a 0.15% additive, which is attributed to improved interfacial bonds

**Table 2.** Processing parameters

Material	Cylinder zone temperatures [°C]				Mold	Pressure in the	
iviaterial	I	Ш	III	IV	temperature [°C]	clamping phase [MPa]	
All compositions	175	185	195	200	60	100	

Table 3. Sample description

Sample	Description
PT	Reference sample – Polyoxymethylene (POM-C; Tarnoform 500 CE) with 2wt% Titanium (IV) oxide, 98+%, anarase powder; Size: <1000 ppm (1 nm); manufacturer: Acros Organics B.V.B.A.a part of Thermo Fisher Scientific (Waltham, MA, USA);
PTSM10	Polyoxymethylene (POM-C; Tarnoform 500 CE) with 2wt% Titanium (IV) oxide, 98+%, anarase powder; Size: <1000 ppm (1 nm); manufacturer: Acros Organics B.V.B.A.a part of Thermo Fisher Scientific (Waltham, MA, USA); with 10wt% Silicone Masterbatch Dow Corning MB40-006, DuPoint (Wilmington, Delaware, USA)
PTSM20	Polyoxymethylene (POM-C; Tarnoform 500 CE) with 2wt% Titanium (IV) oxide, 98+%, anarase powder; Size: <1000 ppm (1 nm); manufacturer: Acros Organics B.V.B.A.a part of Thermo Fisher Scientific (Waltham, MA, USA); with 20wt% Silicone Masterbatch Dow Corning MB40-006, DuPoint (Wilmington, Delaware, USA)
PTAFS5S5	Polyoxymethylene (POM-C; Tarnoform 500 CE) with 2wt% Titanium (IV) oxide, 98+%, anarase powder; Size: <1000 ppm (1 nm); manufacturer: Acros Organics B.V.B.A.a part of Thermo Fisher Scientific (Waltham, MA, USA); with 5wt% aramid fibers PARA-ARAMID FIBERS Product Code Prefix: PASTD-015ERH, size: 1 mm, Minifibers Inc (Johnson City, TN, USA) with 5wt% SCONA TSPOE 1002 GBLL BYK, Additives and Instruments (Wesel, Germany)
PTAFL5S5	Polyoxymethylene (POM-C; Tarnoform 500 CE) with 2wt% Titanium (IV) oxide, 98+%, anarase powder; Size: <1000 ppm (1 nm); manufacturer: Acros Organics B.V.B.A.a part of Thermo Fisher Scientific (Waltham, MA, USA); with 5wt% aramid fibers PARA-ARAMID FIBERS Product Code Prefix: PASTD-015ERH, size: 3 mm, Minifibers Inc (Johnson City, TN, USA), with 5wt% SCONA TSPOE 1002 GBLL BYK, Additives and Instruments (Wesel, Germany)

and enhanced stress transfer [42]. In turn, Liu et al. documented that the introduction of aramid bonding yarn into hybrid composites increased impact resistance by up to 92.7% [43]. Silicone additives were selected on the basis of characteristic indicators that are used as modifiers for polyoxymethylene. The content of the silicon additive was 5 %. This content was selected on the basis of the matweb.com database, which analyzed the compositions of commercial polyoxymethylene composites produced by the largest manufacturers such as: Mitsubishi, BASF, Chem Polymer, Delrin, DuPont, Celanese and others [44].

# **Determination of density**

The density of the produced composites was assessed utilizing the hydrostatic weighing method in accordance with PN-EN ISO 1183 [45]. An electronic analytical balance, specifically the RADWAG AS 220 with a reading accuracy of 0.1 mg (Radwag, Radom, Poland), was used for the measurement, with ethanol at a concentration of 96% serving as the standard liquid.

# Mechanical analysis

The properties derived from the static tensile and hysteresis tests were determined in accordance with the PN-EN ISO 527-1:2019 [46–47] standard, using the MTS Criterion Model 43 testing

machine (MTS System Corp., Eden Prairie, MN, USA) equipped with an MTS axial extensometer. During the testing procedure, the specimens were elongated at a rate of 5 mm/min, with the gauge length set to 100 mm. For the analysis of hysteresis loops and dissipation energy, the samples were subjected to cyclic loading and unloading at a rate of 10 mm/min. The maximum excitation force applied was set at 60% of the force required to fracture the specimen, as determined during the tensile test. The bending properties were assessed using a Shimadzu AGS-X 10 kN testing machine (Kyoto, Japan) with TRAPEZIUM-X software, operating at a test speed of 10 mm/min and a support span of 64 mm. This test was conducted in accordance with the PN-EN ISO 178:2019 standard [48]. Charpy impact stresses were evaluated using a Zwick/Roell HIT5.5P hammer (Ulm, Germany), with measurements conducted in accordance with PN-EN ISO 179-2:2020 [49] on notched samples. The presented test results are the average of at least five tests.

### Optical and scanning electron microscopy

To assess the microstructure of the antimicrobial nanocomposites post-tensile testing, micrographs were captured using the Jeol JSM-IT200 electron microscope (Tokyo, Japan) under vacuum conditions at 15 kV. Images of the specimens were obtained at magnifications of 500x and 1000x.

Prior to placement in the microscope chamber, the composites were coated with gold particles utilizing a sputtering machine, specifically the DII-29030SCTR model (Jeol, Tokyo, Japan).

# Surface characteristics of the sample

The wettability of the surface was assessed using the sitting drop method with the Advex Instruments See System goniometer (Brno, Czech Republic). This procedure adhered to the PN-EN ISO 19403-2:2024 standard [50]. The shape of the drop was captured with a digital camera, transferred to a computer for enlargement, and subsequently analyzed using the See System 7.6 software. The contact angle of the samples was evaluated for three distinct liquids: distilled water, paraffin, and diiodomethane. Surface tension measurements were conducted in accordance with the PN-EN ISO 19403-3:2024 [51] standard, employing the Owens and Wendt method.

#### **RESULTS**

# Physical and mechanical properties

Upon analyzing the variations in sample density, it is evident that the incorporation of silicone and aramid fibers, along with a compatibilizer, results in a slight decrease. Table 4 presents the fundamental properties. The introduction of silicone-based modifiers and aramid fibers leads to a reduction in tensile strength. The most significant decrease in tensile strength, by 28%, accompanied by a 19% reduction in modulus value, was observed in the composites containing 20% MULTIBASETM MB50-011 (PTSM20). The inclusion of 5% aramid fibers resulted in a deterioration of tensile strength by approximately 12% for both fiber lengths. Regarding Young's modulus, the

addition of short aramid fibers increased it by approximately 700 MPa, whereas the inclusion of long fibers resulted in a 277 MPa decrease in the Young's modulus of the composite.

Composite materials incorporating aramid fibers exhibit enhanced stiffness, while the inclusion of high molecular weight silicone additives increases the strain value by approximately 40%. However, these modifiers adversely affect the bending strength of the composites. A significant reduction was observed in the composite containing 20% by weight of high-molecular-weight silicone, where the strength decreased by 20% and the modulus by 15%. For the other specimens, the flexural strength showed a slight decline, with values remaining relatively consistent. In the composites with aramid fibers, the flexural strength was measured at 61 MPa for shorter fibers and 62 MPa for longer fibers. The modulus of elasticity for the former decreased by approximately 123 MPa, while the latter remained comparable to the reference PT sample. The application of silicone modifiers resulted in a reduction in impact strength as the quantity of additive increased. This deterioration in properties may be attributed to the incompatibility between the POM matrix and silicone modifiers or the agglomeration of additives. Additionally, the molecular structure of polyoxymethylene is prone to poor interfacial adhesion between the POM matrix and the rubber phases [33, 34]. In the case of composites with aramid fibers, it was observed that the impact strength slightly decreased for short fibers, whereas it increased by about 20% for long fibers. This phenomenon underscores the importance of selecting appropriate aramid fibers. Certain fibers exhibit a tendency to agglomerate, or their surface characteristics may result in incompatibility with the polymer matrix. This incompatibility can lead to a deterioration of mechanical properties [13].

Table 4. Density and mechanical properties of produced composites with the addition of modifiers

Sample	Density [g/cm³]	Tensile strength [MPa]	Young's modulus E [MPa]	Stain at Ultimate Strength [%]	Flexural strength σm [MPa]	Modulus at bending E [MPa]	Impact strength [J/m³]
Tarnoform 500	1.410 ± 0.01	64.0	2800	-	-	2500	64 ± 3
CE	1.410 ± 0.01	04.0					
PT	1.411 ± 0.01	58.8 ± 1	3262 ± 358	6.0 ± 0.5	68.5 ± 2	1951 ± 72	39 ± 5
PTSM10	1.382 ± 0.01	45.7 ± 2	2807 ± 210	7.2 ± 1.0	64.2 ± 3	1924 ± 110	34 ± 2
PTSM20	1.365 ± 0.01	40.6 ± 1	2642 ± 150	5.4 ± 0.2	55.1 ± 1	1664 ± 57	32 ± 4
PTAFS5S5	1.389 ± 0.01	44.0 ± 1	4009 ± 213	4.5 ± 0.5	61.4 ± 1	1838 ± 65	36 ± 2
PTAFL5S5	1.371 ± 0.01	49.4 ± 2	2985 ± 115	6.6 ± 0.3	61.5 ± 1	1958 ± 120	47 ± 8

# Mechanical energy dissipation

The determination of mechanical hysteresis loops facilitates a comprehensive evaluation of energy losses in materials. In unmodified materials, these processes are predominantly associated with energy dissipation resulting from internal friction between macromolecules. Conversely, in composite materials, energy dissipation during deformation arises not only from classical friction processes but also from additional phenomena

occurring between the components of the composite. These phenomena include losses due to fiber pull-out from the matrix, as well as processes occurring in regions of defects, damage, and areas subjected to internal stress [52]. Figures 1–4 depict the effects of energy dissipation observed during initial mechanical hysteresis loops. The analysis of the final results indicates that the incorporation of silicone-based modifiers reduces stiffness and enhances the capacity for energy dissipation. This relationship becomes more

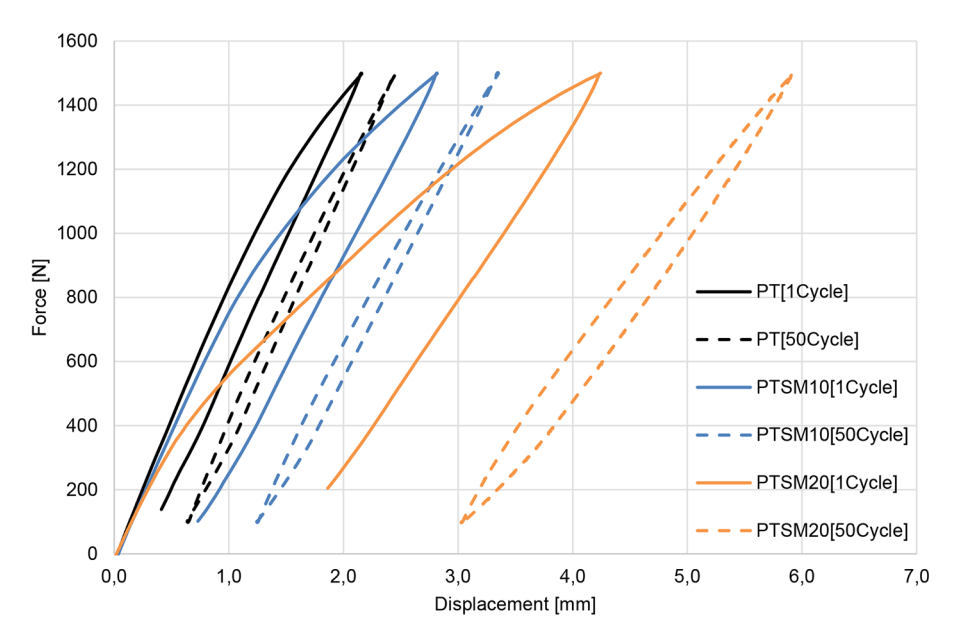


**Figure 1.** Comparison of energy dissipation loops for 1 and 50 cycles of antibacterial POM-based composites with high molecular weight silicone

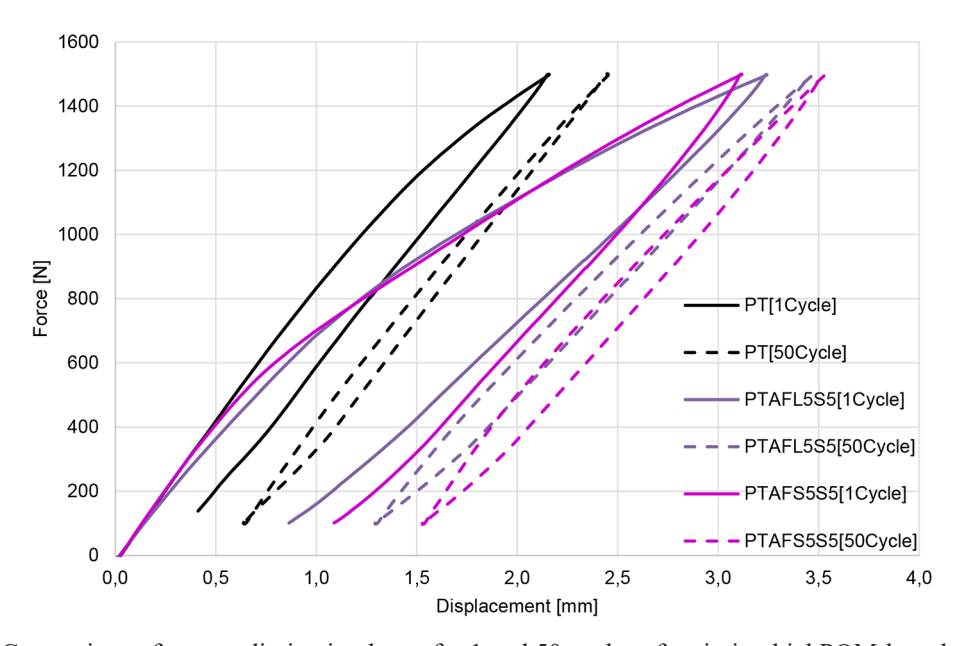


**Figure 2.** Comparison of energy dissipation loops for 1 and 50 cycles of antimicrobial POM-based composites with aramid fiber and compatibilizer

pronounced with an increased amount of additive in the composite. The composites incorporating aramid fibers also exhibit reduced stiffness compared to the base antibacterial PT composite.

Figure 3 shows the dynamic creep diagram of the samples subjected to cyclic loading. A composite with 20% silicone has the highest increase in displacement, which can cause it to fail when fatigue loads are applied to it.

# Morphology of surface

The topography of the cracks observed after the bending test was examined using scanning electron microscopy (SEM). Figure 5 presents micrographs of the composites at x500 and x1000 magnifications. In the composites containing silicone additives, specifically PTSM10 and PTSM20, the presence of defects in the form of

pores is evident, potentially attributable to the incompatibility between the polymer matrix and the silicone additive [32–34]. The quantity of pores increases proportionally with the amount of silicone additive incorporated, a phenomenon corroborated by a reduction in mechanical strength.

Silicone additives in polymer composites have been extensively investigated for their impact on microstructure and mechanical properties. Research indicates that increased silicone content promotes pore formation within the matrix, resulting in diminished mechanical strength due to the pores serving as stress concentration sites. The incorporation of silicone into a polymer matrix frequently leads to phase separation. The chemical incompatibility between silicone and the matrix fosters the development of distinct domains, which transform into microporous structures during the curing process. An elevated

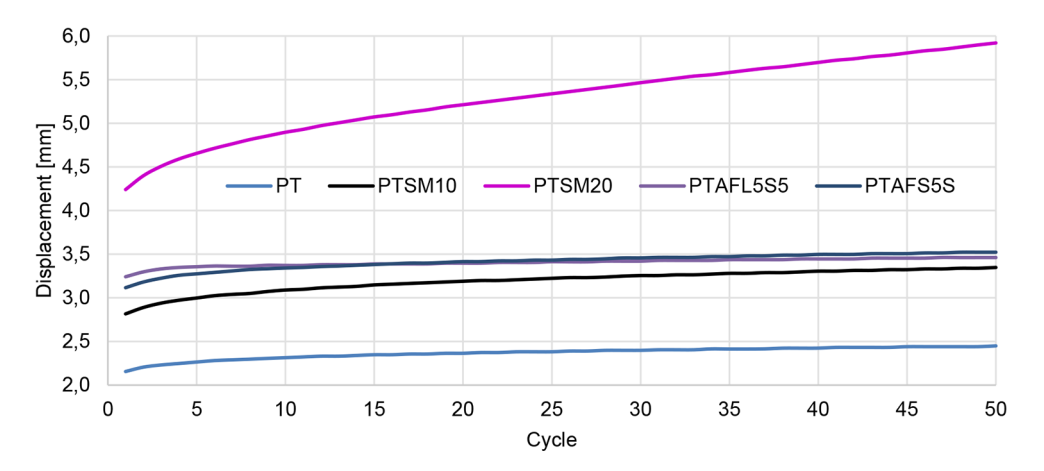
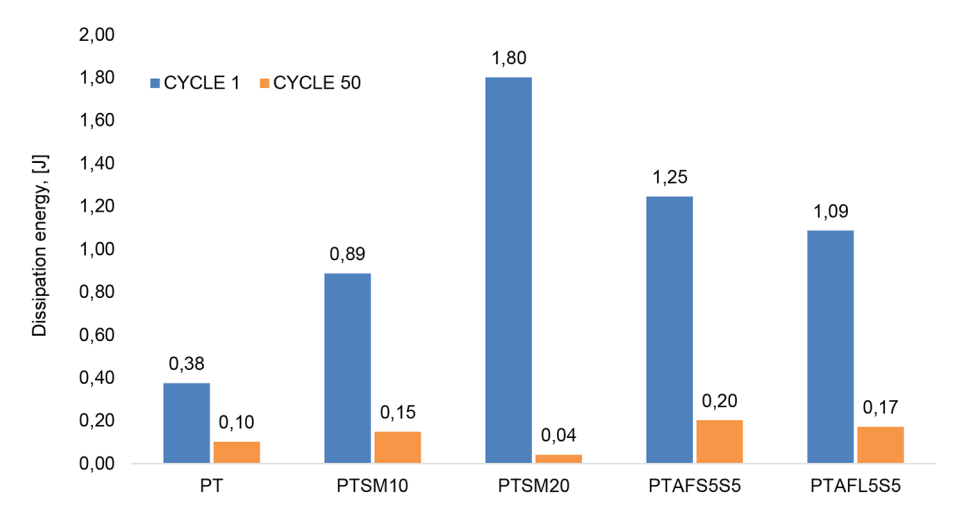


Figure 3. Maximum displacement as a function of the cycles number



**Figure 4.** Comparison of dissipation energy values in the first and fiftieth hysteresis loop for antibacterial composites with modifiers

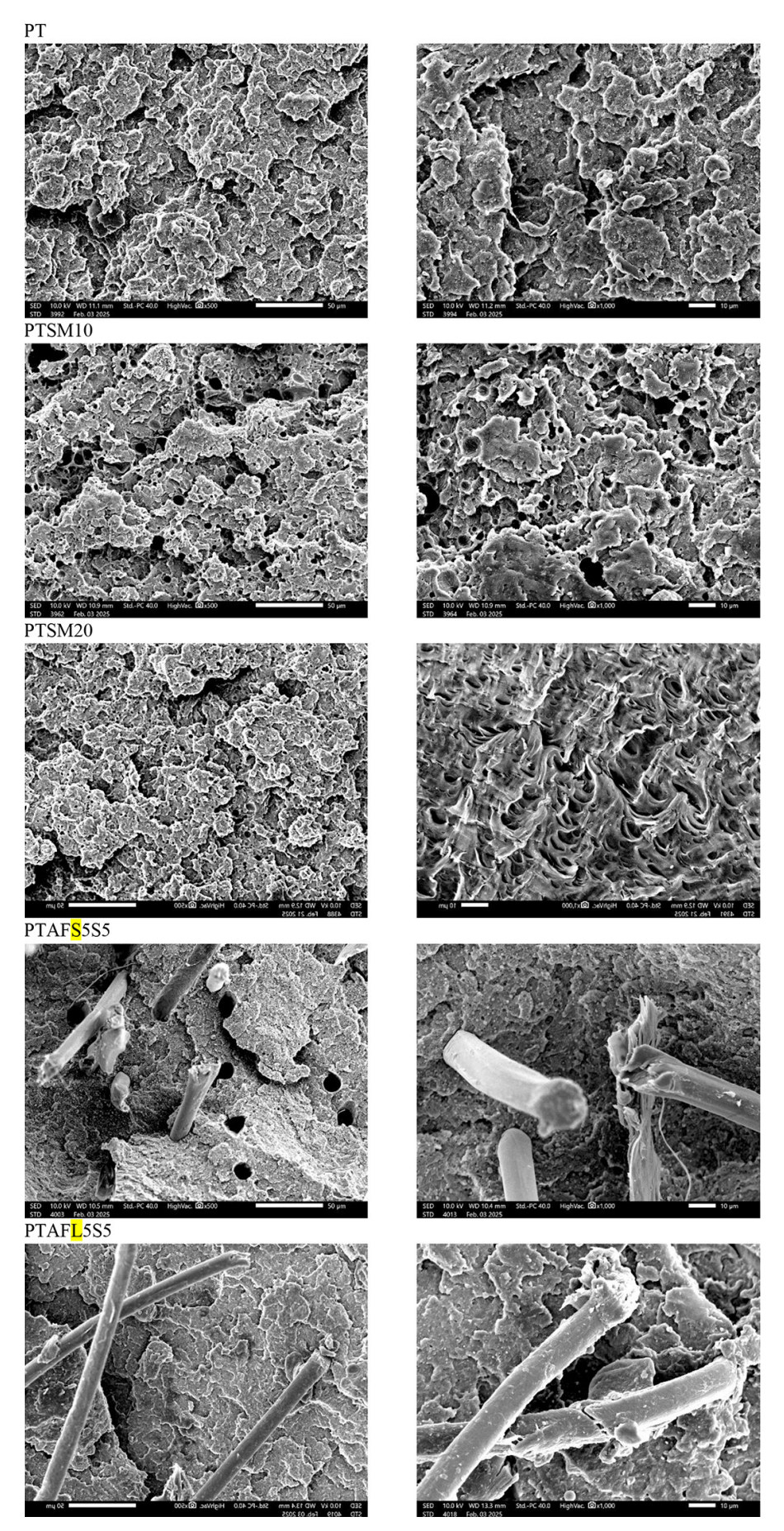


Figure 5. SEM micrographs of the polyoxymethylene based composites after tensile test

additive content exacerbates interfacial instability, leading to an increased number of voids within the material. The presence of pores restricts the load-bearing cross-section of the composite, thereby reducing its stiffness and load resistance. Experimental data demonstrate that key parameters, such as tensile, compressive, and bending strength decline as porosity increases. This phenomenon is well elucidated by fracture mechanics, which posits that structural defects facilitate the initiation and propagation of cracks. Quantitative analyses confirm the proportional relationship between the quantity of silicone additive and the level of porosity, as well as the reduction in mechanical strength. Although silicone enhances the flexibility and processing properties of composites, its influence on the microstructure necessitates careful control. Optimization strategies may include selecting the appropriate additive concentration, employing compatibilizers to improve interfacial adhesion, and controlling processing parameters such as mixing, curing, or heat treatment [53–55].

SEM images revealed structural differences in aramid fibers between PTAFS5S5 and PTAFL5S5 samples. The short fiber composite exhibits a very smooth texture, indicating that despite the application of a 5% compatibilizer, the issues related to fiber-matrix separation persist. Specific voids are observable due to fiber pull-out efect, which compromises the mechanical properties of the composite [17]. Conversely, in PTAFL5S5 samples, the fibers display a less

smooth structure, and the addition of a compatibilizer mitigated this issue, resulting in enhanced impact strength [18–20].

# Contact angle and surface tension

According to the findings, the PT composite exhibits properties similar to those of a hydrophobic polymer, characterized by a contact angle of 82° (Figure 6). Typically, hydrophobic materials possess a contact angle ranging from 90° to 180° [56]. The incorporation of silicone-based modifiers resulted in a significant increase in the contact angles for both water and paraffin. The most favorable outcome for water-composite and paraffin-composite interactions was observed in the PTSM20 samples, where surface wettability was reduced by approximately 50%, in comparison to the PT sample (Table 5).

The highest surface tension was observed in samples incorporating aramid fibers, which resulted in an increase of approximately 4% to 5%. Conversely, the inclusion of silicone led to a reduction in surface tension by 11% to 18%.

## **DISCUSSION**

In prior research, the authors investigated the antibacterial properties of POM matrix composites modified with commonly used biocidal additives, including silver nanoparticles, zinc oxide, copper oxide, and, notably, titanium oxide.

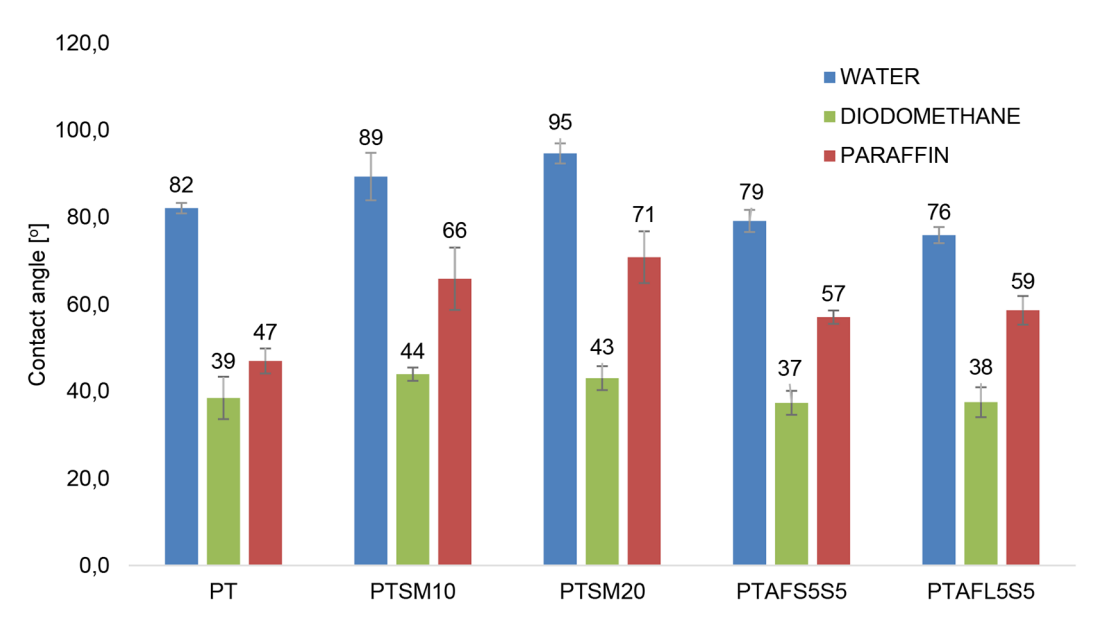


Figure 6. Contact angle values of samples for liquids: water, paraffin and diiodomethane

Table 5. Surface tension

Sample	γ <sub>s</sub> [mJ/m^2]	γ <sub>s</sub> LW [mJ/m^2]	γ <sub>s</sub> AB [mJ/m^2]
PT	43.03	40.34	2.69
PTSM10	38.85	37.55	1.3
PTSM20	38.44	38.05	0.41
PTAF <sub>s</sub> 5S5	44.39	40.89	3.5
PTAF,5S5	45.47	40.82	4.65

The findings indicated that among the additives tested, titanium oxide (TiO2) exhibited the highest antibacterial efficacy, achieving a 100% reduction in Escherichia coli and approximately a 96% reduction in Staphylococcus aureus. This significant activity is attributed to capacity of TiO2 to generate reactive oxygen species and its crystal structure, which facilitates a photocatalytic effect, thereby enhancing its biocidal properties. Notably, the TiO2-infused composites retained their advantageous mechanical properties and demonstrated resistance to aging processes, rendering them particularly promising as structural materials with antimicrobial capabilities, especially for medical industry applications. In contrast, zinc oxide (ZnO) demonstrated moderate antibacterial activity, with a 68% reduction in E. coli and only a 29% reduction in S. aureus. Silver (Ag) nanoparticles exhibited minimal effect on E. coli and reduced S. aureus by approximately 26%. Copper oxide, in two particle fractions, achieved a maximum reduction of approximately 51% [4]. In this study, the authors extend their investigation into polyoxymethylene-titanium oxide composites. The findings presented encompass the physical, mechanical, and dynamic properties of these materials. The incorporation of TiO2 nanoparticles into the base POM matrix enhances biocidal properties, albeit with a slight reduction in mechanical strength. TiO2 is renowned for its photocatalytic activity; under UV radiation, it generates reactive oxygen species (ROS) that deactivate various microorganisms. This effect has been substantiated in numerous studies, demonstrating that even a low weight fraction of TiO<sub>2</sub> nanoparticles can significantly reduce microorganisms [57-58]. When integrated into the POM matrix—which itself may contribute redox properties—TiO<sub>2</sub> nanoparticles can synergize with polyoxometalates, thereby enhancing the antimicrobial efficacy of the composite. This integration facilitates self-cleaning surfaces due to the photocatalytic effect and oxidation [57–59].

Conversely, the slight decrease in mechanical strength may be attributed to the challenges in achieving uniform dispersion of nanoparticles, leading to local stress concentrations [60–61]. In POM matrices, inadequate interfacial interactions can promote the formation of microvoids and defects. Consequently, optimizing the balance between biocidal efficacy and mechanical strength necessitates careful adjustment of the TiO<sub>2</sub> content and improved dispersion, potentially through surface treatment or the use of compatibilizers [62–63].

The enhanced hydrophobicity of silicones facilitates the reduced adhesion of biological contaminants, which is advantageous for antibacterial applications, while simultaneously enhancing the dissipation of mechanical energy. The incorporation of silicones into polyoxymethylene composites, resulting in increased energy dissipation and hydrophobicity, can be attributed to their unique structural characteristics. The distinctive chemical and physical properties of silicones are primarily due to their siloxane (Si-O-Si) backbone and non-polar methyl groups, which endow them with dual antibacterial and mechanical functions. High hydrophobicity results in low free surface energy, thereby diminishing the strength of noncovalent interactions between the surface and biomolecules or microorganisms. Consequently, bacteria and proteins exhibit reduced adhesion to silicones, hindering their ability to colonize and form biofilms. The same structural features responsible for hydrophobicity also determine viscoelastic properties, as flexible siloxane chains can move and reorganize under stress, effectively dissipating energy and limiting local damage. This mechanism enhances the resistance of the material to mechanical damage and fatigue, which is crucial for applications requiring durability and bioprotection. Optimization of silicone surfaces, for instance, through chemical treatment, can further enhance antimicrobial properties without compromising mechanical performance. In summary, hydrophobicity reduces the adhesion of biological contaminants, and the mobility of polymer chains promotes energy dissipation, thereby increasing the overall functionality and durability of the material [64].

The incorporation of aramid fibers, particularly those with longer fibers, positively influences the stiffness, as evidenced by an increase in Young's modulus of up to approximately 700 MPa, and enhances impact strength by 20%. This improvement is attributed to the mechanism of fiber pulling and their adhesion to the matrix. The enhancement in the mechanical properties of aramid fiber-reinforced composites under impact loading is primarily due to the elevated surface energy of these fibers. A higher surface energy facilitates improved wettability, ensuring superior contact at the fiber-matrix interface and strengthening interfacial adhesion, thereby promoting robust chemical and physical interactions [65-66]. Well-wetted, more polarized fiber surfaces enable the formation of stronger bonds with the polymer matrix, resulting in more efficient stress transfer during impacts [67-68]. This increased adhesion mitigates premature detachment and interfacial damage, allowing for an even distribution of loads throughout the composite and stable energy attenuation [69]. A reinforced load transfer mechanism enables the aramid fibers to work in conjunction with the matrix, effectively absorbing and dissipating impact energy over a larger area. This is further supported by the inherent strength and ductility of the fibers, which decelerate crack propagation as well as evenly disperse damage [69-72].

Silicone modifiers are observed to reduce tensile strength by up to 28% and flexural strength by 20% when 20% silicone is incorporated, a phenomenon attributed to the agglomeration and inadequate adhesion of the silicone phase to POM. Initially, when silicone modifiers are introduced into the POM matrix at elevated concentrations, they tend to form aggregates, rather than being uniformly dispersed. This agglomeration is a common issue in composites where there is limited chemical compatibility between the modifier and the polymer. The resultant clusters create localized zones that fail to reinforce the matrix uniformly and instead act as stress concentrators under mechanical loads. Consequently, during the application of tensile or bending forces, these aggregates become sites for the initiation and propagation of cracks, thereby compromising the mechanical integrity of the composite [73]. Furthermore, this issue is compounded by the poor interfacial adhesion between the silicone phase and POM. Effective load transfer necessitates a robust bond between the matrix and the filler; however, silicones possess lower polarity and surface energy compared to POM, which weakens the interfacial bonds. In the regions where the silicone phase agglomerates, the absence of a strong bond allows defects to form, which diminishes tensile and flexural strength, as corroborated by Li et al., who noted that poor adhesion facilitates crack development and deteriorates mechanical properties [74]. In conclusion, the presence of aggregates and inadequate adhesion of the silicon phase result in the formation of localized defects, which disrupt uniform stress distribution and limit the capacity of the composite to bear and dissipate loads. This results in a reduction in mechanical properties, particularly evident in tensile and bending tests. Consequently, it is imperative to optimize the dosage of the modifier, enhance its dispersion, and strengthen the interfacial bond to mitigate these adverse effects. The impact of aggregation and adhesion on composite parameters is corroborated by other studies on various polymer systems [75]. The incorporation of silicone modifiers into the polymer matrix introduces a softer, more viscoelastic phase, resulting in a reduction in overall stiffness, as observed in hysteresis loop tests. This decrease in stiffness is attributed to the lower modulus of elasticity of silicone additives compared to the base matrix, which diminishes the resistance of the composite to deformation under load [76]. The silicone phase is characterized by highly elastic polymer chains that can readily change orientation and deform, resulting in a more responsive material. Simultaneously, these intrinsic properties of silicones facilitate significant energy dissipation during cyclic loading. Large hysteresis loops obtained during loading and unloading cycles indicate that a substantial portion of the mechanical energy is consumed by internal friction within the silicon phase. More specifically, silicone deformation involves mechanisms such as chain loosening, molecular rearrangement, and sliding between chains, which convert mechanical work into heat through internal friction [76]. These deformation processes at the molecular level enhance the ability of the composite to absorb and dissipate energy, rendering the material particularly effective in damping applications. Moreover, the energy dissipation mechanism is

not solely due to the viscoelastic nature of silicone but also due to the internal friction generated during deformation. Computational and experimental studies have demonstrated that the dissipated energy is largely related to the interaction and friction between molecular segments, where even minor movements within the silicon phase during cyclic loading contribute to additional damping [77]. Although the introduction of silicone additives impairs stiffness, the increased damping capability can be advantageous in applications where shock absorption and vibration damping are desired.

The biological response to POM composites, particularly in the context of osteointegration, is determined by both the surface characteristics and the internal composition of the composite. While POM is typically regarded as bioinert, the addition of reactive or bioactive fillers can alter its surface chemistry and topography to facilitate bone tissue integration. For instance, the integration of nano-SiO2 into POM matrices has been demonstrated to improve mechanical properties, potentially creating a surface favorable for apatite nucleation, which is essential for osteointegration [78]. These reactive fillers may offer nucleation sites that support the deposition of calcium phosphate layers, akin to the structures found in other bioactive composites intended for bone substitution [79-80]. The impact of the composite surface on the biological response is multifaceted. Surface roughness, chemical composition, and the presence of specific functional groups are all critical in regulating protein adsorption, cell adhesion, and osteoblast differentiation [81]. Composite surfaces that emulate the extracellular matrix (ECM)—such as those with hierarchical micro- and nanostructures—are recognized for enhancing osteoblast adhesion and proliferation [82]. In scaffolds where bioactive fillers, such as hydroxyapatite or bioactive glass, have been incorporated, the surface morphology promotes enhanced adsorption of serum proteins, encouraging the formation of a bone-like apatite layer and accelerating the osteointegration process [83]. While research specifically examining POM composites within the realm of bone tissue engineering remains limited, current insights indicate that strategic modifications to the composite surface may similarly enhance the biological responses of POM-based materials. Furthermore, the chemical characteristics of the composite, including the nature of the incorporated fillers, play a crucial role

in influencing the biological response by enhancing mechanical stability and regulating the local ionic environment. Studies on composite materials have shown that specific pore sizes and chemical compositions can enhance osteoconductivity and osteogenesis, thereby facilitating improved bone tissue integration [84]. By embedding an appropriate concentration of bioactive fillers, such as reactive nano-SiO<sub>2</sub>, within the POM matrix, it is possible to influence local pH and ion release, thus creating an environment that promotes the differentiation of osteoprogenitor cells and supports the deposition of mineralized tissue [85]. Such synergistic strategies—optimizing both the mechanical robustness of the composite and its surface bioactivity—are essential for advancing materials for orthopedic applications.

In conclusion, although POM is inherently bioinert, its composite form can be engineered to induce a favorable biological response through specific modifications of surface properties and the incorporation of bioactive components. By enhancing surface roughness, altering chemical characteristics, and integrating reactive fillers, POM composites can be transformed into the materials that facilitate osteoblast attachment, promote apatite formation, and ultimately achieve improved osteointegration. These strategies parallel those successfully applied in other bone tissue engineering composites [79–80, 82].

Numerous plastics and composites are employed within the medical industry, among which polymethyl methacrylate (PMMA) is notably utilized as bone cement in orthopedic surgery. This is primarily due to its biocompatibility and its capacity to effectively bond implants to bone tissue. However, a significant limitation of PMMA is its restricted mechanical properties, which can lead to the loosening of implants under physiological stress conditions. To enhance the properties of PMMA, extensive research has been conducted over the years on its modification with various additives. Bioactive fillers, such as calcium phosphates ( $\alpha$ -TCP,  $\beta$ -TCP) and hydroxyapatite (HA), have been demonstrated to enhance the biocompatibility of the material, facilitate bone regeneration, and improve load transfer at the cement-bone interface. Nevertheless, the impact of these additives on mechanical strength is contingent upon their type and concentration; while small quantities can reinforce the composite, higher concentrations often result in diminished strength. Additionally, additives that alter the structure and polymerization process, such as vitreous carbon (GC), are utilized. The influence of these additives on the mechanical properties of PMMA is largely dependent on the size and distribution of the particles; fine-grained fillers tend to be neutral or slightly enhance the material, whereas coarser fillers can disrupt the polymerization process, leading to reduced strength [86-88].

In conclusion, the mechanical properties of polymer composites incorporating silicone additives are predominantly influenced by the microstructure of the material and the quality of interfacial interactions. Homogeneous particle dispersion and effective phase compatibilization contribute to enhanced flexibility and mechanical stability. Conversely, silicone agglomeration, inadequate adhesion, and increased porosity, as observed in the presented results, result in the formation of stress concentrators and structural weakening. Current studies, while affirming the impact of additive quantity and distribution on composite properties, are largely confined to short-term analyses, neglecting aging processes under real-world conditions and comprehensive evaluations of the interface and functionality, such as actual antimicrobial activity. Consequently, future research should prioritize long-term durability assessments, advanced microstructural analysis, and the development of more efficient compatibilizers to optimize composite properties and broaden their practical applicability.

#### CONCLUSIONS

This study demonstrated the successful development of innovative POM-based composites modified with TiO2 nanoparticles, high-molecular-weight silicone, and aramid fibers. The experimental results showed that the incorporation of long aramid fibers improved the stiffness of the composites (increase in Young's modulus by ~700 MPa) and enhanced the impact strength by approximately 20%, confirming the importance of strong fiber-matrix adhesion for effective stress transfer. In contrast, increasing the silicone content, particularly at 20%, reduced tensile strength by up to 28% and flexural strength by 20% due to agglomeration and poor interfacial bonding. Dynamic tests demonstrated that silicone modifiers enhanced energy dissipation, with higher additive concentrations amplifying this effect, although at the cost of reduced stiffness. The composites

reinforced with aramid fibers maintained stable energy attenuation during cyclic loading, supporting their suitability for applications requiring durability under dynamic stress. The addition of silicone significantly increased the hydrophobicity of the surface, with a ~50% reduction in wettability compared to the unmodified composite. The composites with aramid fibers exhibited the highest surface tension (up to ~5% increase), while those with silicone showed a reduction of 11-18%. This balance between increased hydrophobicity and surface energy supports improved antiadhesive and antibacterial potential. Overall, the combination of TiO2, aramid fibers, and silicone resulted in a composite material with optimized dynamic and surface performance — capable of effective energy dissipation under cyclic loads while maintaining antibacterial surface characteristics. These findings underscore the crucial role of compatibilizers in enhancing interfacial adhesion and achieving a balance between mechanical strength and durability. The results provide a solid foundation for further industrial applications, particularly in medical and laboratory components requiring long service life as well as high biological resistance.

## **Acknowledgements**

This research was funded by Ministry of Education and Science: implementation doctorate program DWD/5/0234/2021 "Development of composites with increased antistick and biocidal properties produced on a polyoxymethylene (POM) matrix for elements of medical equipment with increased resistance to aging and impact external loads".

# **REFERENCES**

- 1. Lüftl, S., Visakh, P. M., Chandran, S. Polyoxymethylene handbook: structure, properties, applications and their nanocomposites. John Wiley & Sons. 2014.
- Bijelic, A., Aureliano, M., Rompel, A. The antibacterial activity of polyoxometalates: structures, antibiotic effects and future perspectives. Chemical Communications, 2018; 54(10), 1153–1169. https:// doi.org/10.1039/C7CC07549A
- Zeng, Y., Liu, Y., Wang, L., Huang, H., Zhang, X., Liu, Y.,..., Li, Y. Effect of silver nanoparticles on the microstructure, non-isothermal crystallization behavior and antibacterial activity of polyoxymethylene. Polymers, 2020; 12(2), 424. https://doi.

- org/10.3390/polym12020424
- 4. Kaczor, P., Bazan, P., Kuciel, S. Bioactive polyoxymethylene composites: mechanical and antibacterial characterization. Materials, 2023; 16(16), 5718. https://doi.org/10.3390/ma16165718
- Makvandi, P., Wang, C. Y., Zare, E. N., Borzacchiello, A., Niu, L. N., Tay, F. R. Metal-based nanomaterials in biomedical applications: antimicrobial activity and cytotoxicity aspects. Advanced Functional Materials, 2020; 30(22), 1910021. https://doi.org/10.1002/adfm.201910021
- 6. Gu, X., Xu, Z., Gu, L., Xu, H., Han, F., Chen, B., Pan, X. Preparation and antibacterial properties of gold nanoparticles: A review. Environmental Chemistry Letters, 2021; 19, 167–187. https://doi.org/10.1007/s10311-020-01071-0
- Li, S. C., Li, B., Qin, Z. J. The effect of the Nano-ZnO concentration on the mechanical, antibacterial and melt rheological properties of LLDPE/modified Nano-ZnO composite films. Polymer-Plastics Technology and Engineering, 2010; 49(13), 1334–1338. https://doi.org/10.1080/03602559.2010.496431
- 8. Liu, C., Long, C., Chen, L., Liu, J., Cao, T., Zhang, J. Mechanical and tribological properties of short basalt fiber-reinforced polyoxymethylene composites. Polymer, 2016; 40(6), 836–845. https://doi.org/10.7317/pk.2016.40.6.836
- 9. Wang, Y., Wang, X., Wu, D. Mechanical and tribological enhancement of polyoxymethylene-based composites with long basalt fiber through melt pultrusion. Composite Interfaces, 2016; 23(8), 743–761. https://doi.org/10.1080/09276440.2016.1168124
- Wenzhong, N., Kang, Q., Shaofeng, L., Lujie, Z. Mechanical enhancement, morphology, and crystallization kinetics of polyoxymethylene-based composites with recycled carbon fiber. Journal of Thermoplastic Composite Materials, 2016; 29(7), 935–950. https://doi.org/10.1016/j.polymertesting.2019.106209
- 11. Tang, G., Shao, C., Hu, X., Tang, T. The mechanical properties of carbon fiber-reinforced polyoxymethylene composites filled with silaned nano-SiO<sub>2</sub>. Journal of Thermoplastic Composite Materials, 2016; 29(7), 1020–1029. https://doi.org/10.1177/0892705714556828
- 12. Pihtili, H., Tosun, N. (2002). Effect of load and speed on the wear behaviour of woven glass fabrics and aramid fibre-reinforced composites. Wear, 252(11–12), 979–984. https://doi.org/10.1016/S0043-1648(02)00062-5
- 13. Luo, W., Ding, Q., Li, Y., Zhou, S., Zou, H., Liang, M. Effect of shape morphology on mechanical, rheological and tribological properties of polyoxymethylene/aramid composites. Polymer Science Series A, 2015; 57, 209–220. https://doi.org/10.1134/S0965545X15020108
- 14. Stipho, H. D. Repair of acrylic resin denture base

- reinforced with glass fiber. The Journal of Prosthetic Dentistry, 1998; 80(5), 546–550. https://doi.org/10.1016/S0022-3913(98)70030-7
- Dyer, S. R., Lassila, L. V., Jokinen, M., Vallittu, P. K. Effect of fiber position and orientation on fracture load of fiber-reinforced composite. Dental Materials, 2004; 20(10), 947–955. https://doi. org/10.1016/j.dental.2003.12.003
- Arroyo, M., Zitzumbo, R., Avalos, F. Composites based on PP/EPDM blends and aramid short fibres. Morphology/behaviour relationship. Polymer, 2000; 41(16), 6351–6359. https://doi.org/10.1016/ S0032-3861(99)00821-6
- 17. Jiang, Z., Zhang, H., Zhang, Z., Murayama, H., Okamoto, K. Improved bonding between PAN-based carbon fibers and fullerene-modified epoxy matrix. Composites Part A: Applied Science and Manufacturing, 2008; 39(11), 1762–1767. https://doi.org/10.1016/j.compositesa.2008.08.005
- 18. Li, H., Xu, Y., Zhang, T., Niu, K., Wang, Y., Zhao, Y., Zhang, B. Interfacial adhesion and shear behaviors of aramid fiber/polyamide 6 composites under different thermal treatments. Polymer Testing, 2020; 81, 106209. https://doi.org/10.1016/j.polymertesting.2019.106209
- Patterson, B. A., Malakooti, M. H., Lin, J., Okorom, A., Sodano, H. A. Aramid nanofibers for multiscale fiber reinforcement of polymer composites. Composites Science and Technology, 2018; 161, 92–99. https://doi.org/10.1016/j.compscitech.2018.04.005
- Zhang, Y., Yu, C., Chu, P. K., Lv, F., Zhang, C., Ji, J.,..., Wang, H. Mechanical and thermal properties of basalt fiber reinforced poly (butylene succinate) composites. Materials Chemistry and Physics, 2012; 133(2–3), 845–849. https://doi.org/10.1016/j.matchemphys.2012.01.105
- 21. Xiang, D., Gu, C. A study on the friction and wear behavior of PTFE filled with ultra-fine kaolin particulates. Materials Letters, 2006; 60(5), 689–692. https://doi.org/10.1016/j.matlet.2005.09.061
- 22. Fakhar, A., Razzaghi-Kashani, M., Mehranpour, M. Improvements in tribological properties of polyoxymethylene by aramid short fiber and polytetrafluoroethylene. Iranian Polymer Journal, 2013; 22, 53–59. https://doi.org/10.1007/s13726-012-0102-6
- 23. Unal, H., Mimaroglu, A. and Demir, Z. Int. J. Polymer. Mater. Polymer. Biomater., 2010; 59, 808.
- 24. Bazan, P., Nykiel, M., Kuciel, S. Tribo-mechanical properties of composites based on polyoxymethylene reinforced with basalt fiber and silicon carbide whiskers. Polymer Engineering & Science, 2021; 61(2), 600–611. https://doi.org/10.1002/pen.25605
- 25. Rusin-Żurek, K., Kuciel, S., Kurańska, M. The effect of funcionalized ethylene-n-octene copolymer on mechanical properties of bioPET with organic waste fillers. Polimery, 2023; 68(6), 330–336.

- https://doi.org/10.14314/polimery.2023.6.4
- Xanthos, M., Dagli, S. S. Compatibilization of polymer blends by reactive processing. Polymer Engineering & Science, 1991; 31(13), 929–935. https://doi.org/10.1002/pen.760311302
- 27. Uthaman, N., Majeed, A., Pandurangan. Impact modification of polyoxymethylene (POM). e-Polymers, 2006; 6(1), 34. https://doi.org/10.1515/epoly.2006.6.1.438
- 28. Mehrabzadeh, M., Rezaee Alam, D. Study on physical and mechanical properties, thermal behaviour and morphology of polyacetal and polyurethane thermoplastic elastomer blends. Iranian Journal of Polymer Science and Technology, 2000; 13(3). https://doi.org/10.22063/jipst.2000.326
- 29. Gowda, M. S., Hemavathi, A. B., Srinivas, S., Santhosh, G., Siddaramaiah, H. Physico-mechanical, thermal, and tribological studies of polytetrafluoroethylene-filled polyoxymethylene/silicone composites. Journal of Thermoplastic Composite Materials, 2022; 35(6), 846–859. https://doi.org/10.1177/0892705720925117
- 30. Palanivelu, K., Balakrishnan, S., Rengasamy, P. Thermoplastic polyurethane toughened polyacetal blends. Polymer testing, 2000; 19(1), 75–83. https://doi.org/10.1016/S0142-9418(98)00072-5
- 31. Gao, Y., Sun, S., He, Y., Wang, X., Wu, D. Effect of poly (ethylene oxide) on tribological performance and impact fracture behavior of polyoxymethylene/polytetrafluoroethylene fiber composites. Composites Part B: Engineering, 2011; 42(7), 1945–1955. https://doi.org/10.1016/j.compositesb.2011.05.044
- 32. Chen, J., Cao, Y., Li, H. Investigation of the friction and wear behaviors of polyoxymethylene/linear low-density polyethylene/ethylene-acrylicacid blends. Wear, 2006; 260(11–12), 1342–1348. https://doi.org/10.1016/j.wear.2005.09.035
- 33. Wang, X., Cui, X. Effect of ionomers on mechanical properties, morphology, and rheology of polyoxymethylene and its blends with methyl methacrylate—styrene—butadiene copolymer. European Polymer Journal, 2005; 41(4), 871–880. https://doi.org/10.1016/j.eurpolymj.2004.10.046
- 34. Laursen, J. L., Sivebæk, I. M., Christoffersen, L. W., Papsøe, M., Vigild, M. E., Brondsted, P., Horsewell, A. Influence of tribological additives on friction and impact performance of injection moulded polyacetal. Wear, 2009; 267(12), 2294–2302. https://doi. org/10.1016/j.wear.2009.03.048
- 35. Timmons, C. O., Zisman, W. A. The effect of liquid structure on contact angle hysteresis. Journal of Colloid and Interface Science, 1966; 22(2), 165–171. https://doi.org/10.1016/0021-9797(66)90080-4
- 36. Liu, W., Wu, X., Li, Y., Liu, S., Lv, Y., Zhang, C. Fabrication of silver ions aramid fibers and polyethylene

- composites with excellent antibacterial and mechanical properties. e-Polymers, 2022; 22(1), 917–928. https://doi.org/10.1515/epoly-2022-0082
- 37. Bürgers, R., Eidt, A., Frankenberger, R., Rosentritt, M., Schweikl, H., Handel, G., Hahnel, S. The anti-adherence activity and bactericidal effect of microparticulate silver additives in composite resin materials. Archives of Oral Biology, 2009; 54(6), 595–601. https://doi.org/10.1016/j.archoralbio.2009.03.004
- Liang, X., Qin, L., Wang, J., Zhu, J., Zhang, Y., Liu, J. Facile construction of long-lasting antibacterial membrane by using an orientated halloysite nanotubes interlayer. Industrial & Engineering Chemistry Research, 2018; 57(9), 3235–3245. https://doi. org/10.1021/acs.iecr.7b04725
- Chen, S., Wang, Q., Wang, T. Physical properties of aramid fiber reinforced castor oil-based polyurethane/epoxy resin ipn composites. Journal of Reinforced Plastics and Composites, 2013; 32(15), 1136– 1142. https://doi.org/10.1177/0731684413490816
- 40. Pincheira, G., Canales, C., Medina, C., Fernández, E., Flores, P. Influence of aramid fibers on the mechanical behavior of a hybrid carbon–aramid–reinforced epoxy composite. Proceedings of the Institution of Mechanical Engineers Part L Journal of Materials Design and Applications, 2015; 232(1), 58–66. https://doi.org/10.1177/1464420715612827
- 41. Overberg, M., Khurshid, M., Abdkader, A., Hasan, M., Cherif, C. Development of a micro-scale hybridized yarn structure from recycled carbon, aramid and polyamide 6 staple fibers for thermoplastic composites with improved impact strength. Textile Research Journal, 2023; 94(5–6), 636–648. https://doi.org/10.1177/00405175231197652
- 42. Du, X., Kong, H., Xu, Q., Li, B., Yu, M., Li, Z. (2022). Effects of aramid nanofibers on the mechanical properties of epoxy resin and improved adhesion with aramid fiber. Polymer Composites, 43(4), 2103–2114. https://doi.org/10.1002/pc.26524
- 43. Liu, Y., Natsuki, T., Huang, C., Nakajima, T., Xia, H., Ni, Q. Effect of woven structure and aramid binder yarn on the flexural performance of carbon/aramid fiber hybrid three-dimensional woven composites. Polymer Composites, 2022; 43(12), 8831–8849. https://doi.org/10.1002/pc.27065
- 44. https://matweb.com/search/QuickText.aspx?Searc hText=Polyoxymethylene. Access date 26/08/2025
- 45. ISO3167:2014-09; Plastics—Universal Test Specimens. ISO: Geneva, Switzerland, 2014.
- 46. ISO 1183-1:2019 Plastics Methods for determining the density of non-cellular plasticsPart 1: Immersion method, liquid pycnometer method and titration method; Geneva, Switzerland, 2019.
- 47. ISO 527-1:2019; Plastics—Determination of Tensile Properties—Part 1: General Principles. ISO:

- Geneva, Switzerland, 2019.
- 48. ISO 178:2019-06; Plastics—Determination of Bending Properties. ISO: Geneva, Switzerland, 2019.
- 49. ISO 179-2:2020-12; Plastics—Charpy Impact Testing—Part 2: Instrumental Impact Testing. ISO: Geneva, Switzerland, 2020.
- 50. ISO 19403-2:2024: Determination of the surface free energy of solid surfaces by measuring the contact angle. ISO: Geneva, Switzerland, 2024.
- 51. ISO 19403-3:2024: Determination of the surface tension of liquids using the pendant drop method. ISO: Geneva, Switzerland, 2024.
- 52. Shrestha, R., Simsiriwong, J., Shamsaei, N. Mean strain effects on cyclic deformation and fatigue behavior of polyether ether ketone (PEEK). Polymer testing, 2016; 55, 69–77. https://doi.org/10.1016/j. polymertesting.2016.08.002
- 53. Smith, J. A., Doe, A. B. Effects of silicone additives on the microstructure and mechanical properties of polymer composites. Journal of Composite Materials, 2008; 42(9), 987–995. https://doi.org/10.1177/0021998308093651
- 54. Lee, C. K., Nguyen, T. Q. Phase separation and pore formation in silicone-modified polymer matrices. Polymer Engineering & Science, 2010; 50(3), 500–508. https://doi.org/10.1002/pen.21075
- 55. Zhang, Y., et al. Impact of silicone additive levels on structure-property relationships in polymer composites. Composite Science and Technology, 2012; 72(5), 666–673. https://doi.org/10.1016/j.compscitech.2011.12.012
- 56. Law, K. Y. Definitions for hydrophilicity, hydrophobicity, and superhydrophobicity: getting the basics right. The Journal of Physical Chemistry Letters, 2014; 5(4), 686–688.
- 57. Zapata, P., Palza, H., Delgado, K., Rabagliati, F. Novel antimicrobial polyethylene composites prepared by metallocenic in situ polymerization with tio2-based nanoparticles. Journal of Polymer Science Part a Polymer Chemistry, 2012; 50(19), 4055–4062. https://doi.org/10.1002/pola.26207
- Zenteno, A., Guerrero, S., Ulloa, M., Palza, H., Zapata, P. Effect of hydrothermally synthesized titanium nanotubes on the behaviour of polypropylene for antimicrobial applications. Polymer International, 2015; 64(10), 1442–1450. https://doi.org/10.1002/pi.4939
- 59. Fonseca, C., Ochoa, A., Ulloa, M., Álvarez, E., Canales, D., Zapata, P. Poly(lactic acid)/tio2 nanocomposites as alternative biocidal and antifungal materials. Materials Science and Engineering C, 2015; 57, 314–320. https://doi.org/10.1016/j. msec.2015.07.069
- Wacharawichanant, S., Sangkhaphan, A., Sa-Nguanwong, N., Khamnonwat, V., Thongyai, S., Praserthdam, P. Effects of particle type on thermal and

- mechanical properties of polyoxymethylene nanocomposites. Journal of Applied Polymer Science, 2011; 123(6), 3217–3224. https://doi.org/10.1002/app.34984
- 61. Zhao, H., Ma, W., Zhang, L., Cui, L., Sun, B., Wu, M., ..., Du, Y. Tio2-loaded epoxy resin with improved electrical characteristics as promising insulating materials. Plastics Rubber and Composites Macromolecular Engineering, 2020; 49(4), 179–186. https://doi.org/10.1080/14658011.2020.1723315
- 62. Zhou, F., Wang, D., Zhang, J., Li, J., Lai, D., Lin, S., ..., Hu, J. Preparation and characterization of biodegradable κ-carrageenan based anti-bacterial film functionalized with wells-dawson polyoxometalate. Foods, 2022; 11(4), 586. https://doi.org/10.3390/foods11040586
- 63. Tajdari, A., Babaei, A., Goudarzi, A., Partovi, R., Rostami, A. Hybridization as an efficient strategy for enhancing the performance of polymer nanocomposites. Polymer Composites, 2021; 42(12), 6801–6815. https://doi.org/10.1002/pc.26341
- 64. Bazan, P., Kuciel, S., Nykiel, M. Characterization of composites based on polyoxymethylene and effect of silicone addition on mechanical and tribological behavior. Polymer Engineering & Science, 2019; 59(5), 935–940.
- 65. Hao, W., Yao, X., Ke, Y., Ma, Y., Li, F. Experimental characterization of contact angle and surface energy on aramid fibers. Journal of Adhesion Science and Technology, 2013; 27(9), 1012–1022. https://doi.org/10.1080/01694243.2012.727172
- 66. Wang, J., Chen, P., Xiong, X., Jia, C., Yu, Q., Ma, K. Interface characteristic of aramid fiber reinforced poly(phthalazinone ether sulfone ketone) composite. Surface and Interface Analysis, 2017; 49(8), 788–793. https://doi.org/10.1002/sia.6224
- 67. Xie, F., Xing, L., Liu, L., Liu, Y., Zhong, Z., Jia, C., ..., Huang, Y. Surface ammonification of the mutual-irradiated aramid fibers in 1,4-dichlorobutane for improving interfacial properties with epoxy resin. Journal of Applied Polymer Science, 2017; 134(23). https://doi.org/10.1002/app.44924
- 68. Lu, C., Wang, J., Wang, H., Shang, K. Enhancing interfacial adhesion: deprotonation and mussel-inspired coating of aramid fibers. Acs Applied Polymer Materials, 2024; 6(14), 8048–8055. https://doi. org/10.1021/acsapm.4c00723
- 69. Özsoy, M. Investigation of the energy absorption behavior and damage mechanisms of aramid/carbon/jute fiber hybrid epoxy composites. Polymer Composites, 2024; 45(12), 11515–11531. https:// doi.org/10.1002/pc.28583
- Gore, P. and Kandasubramanian, B. Functionalized aramid fibers and composites for protective applications: a review. Industrial & Engineering Chemistry Research, 2018; 57(49), 16537–16563. https://doi.

- org/10.1021/acs.iecr.8b04903
- Pach, J., Pawłowska, A. Quasi-static penetration properties of hybrid composites with aramid, carbon and flax fibers as reinforcement. Advances in Science and Technology Research Journal, 2024; 18(6), 304– 320. https://doi.org/10.12913/22998624/192152
- Szczepaniak, R., Przybyłek, P., Krzysztofik, K. Effect of the amount and location of phase change materials in a fibre reinforced composite matrix on ablative properties. Advances in Science and Technology Research Journal, 2025; 19(3), 228–237. https://doi.org/10.12913/22998624/196965
- Dasari, A., Zhang, Q., Yu, Z., Mai, Y. Toughening polypropylene and its nanocomposites with submicrometer voids. Macromolecules, 2010; 43(13), 5734–5739. https://doi.org/10.1021/ma100633y
- 74. Li, Y., Zhang, Y., Zhang, Y. Mechanical properties of high-density polyethylene/scrap rubber powder composites modified with ethylene–propylene–diene terpolymer, dicumyl peroxide, and silicone oil. Journal of Applied Polymer Science, 2003; 88(8), 2020–2027. https://doi.org/10.1002/app.11907
- Wong, F. and Adnan, U. Mechanical properties of rice husk-recycled polypropylene composite. Journal of Mechanical Engineering, SI 2023; 12(1), 45– 61. https://doi.org/10.24191/jmeche.v12i1.24637
- 76. Li, Z., Mao, Z., Wang, B., Li, T. Molecular origins of shock dissipation in polymer-based nanocomposites. The Journal of Physical Chemistry B, 2024; 128(9), 2201–2214. https://doi.org/10.1021/acs. jpcb.3c08071
- 77. Premnath, M. and Gopi, K. Experimental and numerical analysis of the performance of various damper materials. Trends in Sciences, 2023; 20(8), 5038. https://doi.org/10.48048/tis.2023.5038
- 78. Xu, X., Guo, L., Zhang, Y., Zhang, Z. Mechanical and thermal properties of reactable nanosio<sub&gt;2&lt;/sub&gt;/polyoxymethylene composites. Advanced Materials Research, 2012; 535–537, 103–109. https://doi.org/10.4028/www.scientific.net/amr.535-537.103
- 79. Yang, C., Wang, Y., Chen, X. Preparation and evaluation of biomimetric nano-hydroxyapatite-based composite scaffolds for bone-tissue engineering. Chinese Science Bulletin, 2012; 57(21), 2787–2792. https://doi.org/10.1007/s11434-012-5201-4
- 80. Reis, E., Borges, A., Carlo, R., Martínez, M., Oliveira, P., Morato, G., ..., Reis, M. Comparison of in vivo properties of hydroxyapatite-polyhydroxybutyrate

- composites assessed for bone substitution. Journal of Craniofacial Surgery, 2009; 20(3), 853–859. https://doi.org/10.1097/scs.0b013e3181a14c30
- Vagaská, B., Bačáková, L., Filová, E., Balík, K. Osteogenic cells on bio-inspired materials for bone tissue engineering. Physiological Research, 2010; 309–322. https://doi.org/10.33549/physiolres.931776
- 82. Kim, J., Han, Y., Lee, H., Kim, J., Kim, Y. Effect of morphological characteristics and biomineralization of 3d-printed gelatin/hyaluronic acid/hydroxyapatite composite scaffolds on bone tissue regeneration. International Journal of Molecular Sciences, 2021; 22(13), 6794. https://doi.org/10.3390/ijms22136794
- 83. Lu, H., El-Amin, S., Scott, K., Laurencin, C. Threedimensional, bioactive, biodegradable, polymer–bioactive glass composite scaffolds with improved mechanical properties support collagen synthesis and mineralization of human osteoblast-like cells in vitro. Journal of Biomedical Materials Research Part A, 2003; 64A(3), 465–474. https://doi.org/10.1002/jbm.a.10399
- 84. Nadezhdin, S., Zubareva, E., Burda, Y., Kolobov, Y., Ivanov, M., Khramov, G., ..., Afanas'ev, A. Influence of implants surface properties on bone tissue formation in the ectopic osteogenesis test. Bulletin of Experimental Biology and Medicine, 2017; 162(6), 812–814. https://doi.org/10.1007/s10517-017-3719-9
- 85. Stodolak-Zych, E., Frączek-Szczypta, A., Błażewicz, M., Błażewicz, S. Composites for bone surgery based on micro- and nanocarbons. Acta Physica Polonica A, 2010; 118(3), 450–456. https://doi.org/10.12693/aphyspola.118.450
- 86. Karpiński, R., Szabelski, J., Krakowski, P., Jonak, J., Falkowicz, K., Jojczuk, M.,..., Przekora, A. Effect of various admixtures on selected mechanical properties of medium viscosity bone cements: Part 1–α/β tricalcium phosphate (TCP). Composite Structures, 2024; 343, 118306.
- 87. Karpiński, R., Szabelski, J., Krakowski, P., Jonak, J., Falkowicz, K., Jojczuk, M.,..., Przekora, A. Effect of various admixtures on selected mechanical properties of medium viscosity bone cements: Part 2–Hydroxyapatite. Composite Structures, 2024; 343, 118308.
- 88. Karpiński, R., Szabelski, J., Krakowski, P., Jonak, J., Falkowicz, K., Jojczuk, M.,..., Przekora, A. Effect of various admixtures on selected mechanical properties of medium viscosity bone cements: Part 3–Glassy carbon. Composite Structures, 2024; 343, 118307.